Growth Hormone Secretion Is Correlated With Neuromuscular Innervation Rather Than Motor Neuron Number in Early-Symptomatic Male Amyotrophic Lateral Sclerosis Mice

F. J. Steyn,* K. Lee,* M. J. Fogarty, J. D. Veldhuis, P. A. McCombe, M. C. Bellingham, S. T. Ngo,* and C. Chen*

School of Biomedical Sciences (F.J.S., K.L., M.C.B., S.T.N., C.C.), University of Queensland, St Lucia, Queensland, Australia, 4072; Centre of Advanced Light Microscopy (M.J.F.), School of Biomedical Sciences, University of Queensland, St Lucia, Queensland, Australia, 4072; Department of Medicine (J.D.V.), Endocrine Research Unit, Mayo School of Graduate Medical Education, Clinical Translational Science Center, Mayo Clinic, Rochester, Minnesota 55905; Department of Neurology (P.A.M.), Royal Brisbane and Women's Hospital, Herston, Queensland, Australia; and University of Queensland Centre for Clinical Research (P.A.M., S.T.N.), University of Queensland, Herston, Queensland, Australia, 4006

GH deficiency is thought to be involved in the pathogenesis of amyotrophic lateral sclerosis (ALS). However, therapy with GH and/or IGF-I has not shown benefit. To gain a better understanding of the role of GH secretion in ALS pathogenesis, we assessed endogenous GH secretion in wild-type and hSOD1^{G93A} mice throughout the course of ALS disease. Male wild-type and hSOD1^{G93A} mice were studied at the presymptomatic, onset, and end stages of disease. To assess the pathological features of disease, we measured motor neuron number and neuromuscular innervation. We report that GH secretion profile varies at different stages of disease progression in hSOD1^{G93A} mice; compared with age-matched controls, GH secretion is unchanged prior to the onset of disease symptoms, elevated at the onset of disease symptoms, and reduced at the end stage of disease. In hSOD1^{G93A} mice at the onset of disease, GH secretion is positively correlated with the percentage of neuromuscular innervation but not with motor neuron number. Moreover, this occurs in parallel with an elevation in the expression of muscle IGF-I relative to controls. Our data imply that increased GH secretion at symptom onset may be an endogenous endocrine response to increase the local production of muscle IGF-I to stimulate reinnervation of muscle, but that in the latter stages of disease this response no longer occurs. **(*Endocrinology* 154: 4695–4706, 2013)**

Amyotrophic lateral sclerosis (ALS) is a neurodegenerative disease characterized by the loss of upper and lower motor neurons. Progression of the disease results in paralysis and death (1, 2). Although disease etiology remains to be wholly understood, studies suggest that ALS is a multifactorial disease, whereby abnormal protein function (3–8), excitotoxicity (1, 9), mitochondrial dysfunction (10–12), and defective metabolic homeostasis (13–15) are thought to contribute to disease progression, and whereby cells such as astrocytes contribute to motor neuron death (16).

The GH/IGF-I axis plays an integral role in the regulation of body metabolism while also stimulating muscle growth (17, 18). Interestingly GH deficiency in human ALS has been thought to play a pathogenic role in the disease process (19–21). Our recent observations confirm GH deficiency and impairment of the GH/IGF-I axis in the hSOD1^{G93A} mouse model of ALS (22). At the latter stage

ISSN Print 0013-7227 ISSN Online 1945-7170
Printed in U.S.A.

Received June 19, 2013. Accepted September 20, 2013.
First Published Online October 9, 2013

* F.J.S. and K.L. contributed equally to this work. S.T.N and C.C contributed equally to this work and are considered senior authors.

Abbreviations: AChR, acetylcholine receptor; ALS, amyotrophic lateral sclerosis; GAPDH, glyceraldehyde-3-phosphate dehydrogenase; GH-R, GH receptor; IGF-IR, IGF-I receptor; IGF-IRα, IGF-I receptor α; IGF-IRβ, IGF-I receptor β; MPP, mass per pulse; NMJ, neuromuscular junctions; SOD1, superoxide dismutase-1; TBS-T, Tris-buffered saline-Tween 20; WT, wild-type.

of disease, hSOD1^{G93A} mice show significant reductions in GHRH-stimulated GH release, decreased pulsatile GH secretion, diminished levels of circulating IGF-I, and lower expression of IGF-I receptor (IGF-IR) in skeletal muscle and spinal cord (22). Collectively, observations in humans and mice suggest that altered endocrine function, at least at the level of the GH/IGF-I axis, coexist with pathological changes in ALS. Although GH/IGF-I directed therapies have been trialed in ALS, the outcomes of these studies were far from promising (21, 23–26). Consequently, there is a need to better understand how, or if, altered GH/IGF-I function contributes to ALS pathogenesis.

To provide insight into the role of GH/IGF-I dysfunction on the onset and progression of ALS, we assessed pulsatile GH secretion and muscle-specific GH receptor (GH-R) expression in hSOD1^{G93A} mice, relative to disease progression. In addition, we measured circulating levels of IGF-I, and muscle-specific IGF-I and IGF-IR expression. When compared with age-matched wild-type (WT) controls, hSOD1^{G93A} mice have higher GH secretion at an age that corresponds to the onset of disease symptoms, when there is loss of motor neurons from the spinal cord. Loss of motor neurons leads to loss of innervation of skeletal muscle neuromuscular junctions (NMJs), which is compensated by reinnervation from other surviving motor neurons (27). GH secretion at this stage of disease was positively correlated with the percentage of NMJs that were innervated, whereas we observed no association between the pulsatile release of GH and crural flexor motor neuron numbers. This suggests that GH plays a role in reinervation of muscle fibers, as compensation for denervation. We also observed higher levels of muscle-specific IGF-I expression in hSOD1^{G93A} mice at the onset of disease, which is indicative of muscle-specific anabolic actions of GH. Secretion of IGF-I by muscle fibers could assist in stimulating sprouting of axon terminals to form new NMJs. This study is the first to document changes in the GH/IGF-I axis relative to disease severity. Our observations suggest that alterations to the GH/IGF-I axis in hSOD1^{G93A} mice may occur as a consequence of the disease process and represents an endogenous response to counteract the muscle atrophy and weakness that is seen in ALS.

Materials and Methods

Animals

WT and hSOD1^{G93A} mice (B6.Cg-Tg[SOD1-G93A]1Gur/J) (28) were bred at the University of Queensland. Founder lines were obtained from The Jackson Laboratory. The SOD1-G93A transgene was designed with a mutant human superoxide dismutase-1 (SOD1) gene, harboring a single amino acid substitution of glycine to alanine (at codon 93). The transgene is driven by the endogenous human SOD1 promoter, resulting in phenotypic changes matching ALS symptoms. Experiments were conducted in male age-matched WT and male hSOD1^{G93A} animals at ages that correspond to well-defined stages of disease progression: prior to the onset of overt symptoms (Presymptomatic; 30–36 d), the onset of hind limb weakness (Onset; 63–75 d), and a latter stage of disease characterized by hind-limb paralysis (End-stage; 150–175 d) (22, 29). Mice were pair-housed (n = 2) in a 12-hour light, 12-hour dark cycle (on at 0600 h and off at 1800 h) and had free access to food (20% protein, 4.8% fat; Specialty Feeds) and water. Room temperature was maintained at 22 ± 2°C. Mice were anesthetized with sodium pentobarbital (ip, 32 mg/kg) prior to the collection of tissue samples. All animal procedures were approved by The University of Queensland Animal Ethics Committee and were performed in accordance with national guidelines.

Experiment 1: Assessment of changes in the GH/IGF-I axis in hSOD1^{G93A} mice relative to disease severity

Measures of pulsatile GH secretion from hSOD1^{G93A} mice were assessed at ages corresponding to presymptomatic, onset, and the end stage of disease (n = 6/age). Observations were compared with age-matched WT controls (n = 8/age). Two weeks prior to the assessment of GH secretion, animals were relocated to the procedure room. Pulsatile GH secretion was assessed as previously described (22, 30). Starting at 0700 hours, 36 sequential tail-tip blood samples were collected from each mouse at 10-minute intervals. All animals had ad libitum access to food and water for the duration of the experiment. Blood loss was restricted to less than 7.5% of total blood volume. Following collection of blood samples, animals were returned to their home cage and allowed 2 days to recover. A subset of animals (n = 5–6/age and genotype) was sacrificed for collection of spinal cord, gastrocnemius, and plasma. Samples were processed for histological verification of disease progression as detailed previously (29), and assessment of hypothalamic somatostatin (Srif) and Ghrh mRNA expression, circulating IGF-I, muscle-specific IGF-I expression, and muscle-specific Gh-r mRNA, and GH-R and IGF-IR protein expression.

Experiment 2: Correlation analysis of pulsatile GH secretion in hSOD^{G93A} mice at disease onset relative to histopathological hallmarks of disease

Pulsatile GH secretion from a second cohort of hSOD1^{G93A} mice at disease onset (n = 16) was measured for correlation between parameters of GH secretion and the histological hallmarks of disease. Given the absence of histological pathology in WT mice, controls (n = 6) were included to confirm altered GH secretion as observed in experiment 1. Assessment of pulsatile GH secretion was performed as described in experiment 1. Following the collection of blood samples, animals were returned to their home cage. After 2 days of recovery, hSOD1^{G93A} mice were sacrificed for collection of the gastrocnemius muscle and spinal cord. Measures of pulsatile GH secretion were compared with the percentage of innervated NMJs of the gastrocnemius muscle (as assessed by percentage acetylcholine receptor [AChR] plaques colocalized with neurofilament and synaptophysin,

n = 16), and the number of neurons in the crural flexor motor neuron pool (L4–L5, n = 12).

Hormone analysis

Circulating IGF-I and IGF-I expression within gastrocnemii were determined using a commercial ELISA (R&D Systems). Analysis of whole blood GH and pituitary GH content was performed using an in-house GH ELISA (30). Muscle tissue and pituitary glands were lysed in buffer: 50 mM Tris-HCl, 150 mM NaCl, 10 mM NaF, 10 mM $Na_4P_2O_4$, 1 mM Na_3VO_4, 1% NP-40, and Protease Inhibitor (Roche). Expression levels of IGF-I in muscle and GH content in pituitary glands were normalized to total protein. The intra- and interassay coefficients of variation for all assays were below 4.50%.

Real-time quantitative PCR

Isolated whole hypothalamic tissue from WT and hSOD1^{G93A} mice at disease onset and gastrocnemius muscles of WT and hSOD1^{G93A} mice at the presymptomatic, onset, and end-stage age were processed for gene expression. Samples were suspended in 1 mL TRIzol (Life Technologies) and stored at −80°C for subsequent analysis. Real-time PCR was conducted as previously described (22). Results were normalized to glyceraldehyde-3-phosphate dehydrogenase (GAPDH). Final measures are presented as relative levels of corrected gene expression compared with expression in controls. For the hypothalamus, mRNA expression was limited to Srif (No. 4331182; Life Technologies) and Ghrh (No. 4331182; Life Technologies) mRNA using commercial TaqMan primers. For gastrocnemius muscles, gene expression was limited to Gh-r mRNA (Catalog No. 4331182; Life Technologies).

Western blotting

Gastrocnemius muscles of WT and hSOD1^{G93A} mice were lysed in buffer (as above). Samples were resolved by SDS-PAGE and transferred to nitrocellulose membranes. Membranes for IGF-I receptor α (IGF-IRα) and IGF-I receptor β (IGF-IRβ) were blocked in 5% skim milk-0.1% Tris-buffered saline-Tween 20 (TBS-T). Membranes for GH-R were blocked in 2.5% BSA-TBS-T. Membranes were incubated overnight with anti-IGF-IRα (1:150 in 2.5% skim milk-TBS-T; sc-712; Santa-Cruz), anti-IGF-IRβ (1:100 in 2.5% skim milk-TBS-T; sc-713; Santa-Cruz), or anti-GH-R (1:1 000 in 1.25% BSA-TBS-T; G8919; Sigma) and detected with donkey antirabbit IgG HRP (1:10 000 in 2.5% skim-milk-TBS-T; NA934; Amersham) or rabbit antigoat IgG HRP (1:20 000 in 1.25% BSA-TBS-T; 81-1620; Invitrogen). Blots were stripped and reprobed with anti-GAPDH (1:15 000 in 2.5% skim-milk-TBS-T; MAB374; Millipore) and detected with sheep antimouse IgG HRP (1:10 000 in 2.5% skim-milk-TBS-T; NA931; Amersham) to verify equal loading of protein. Densitometric analyses of immunoreactive bands were carried out as described previously (22, 31).

Histology for motor neuron counts

Processing and quantification of motor neuron numbers in WT and hSOD1^{G93A} mice were conducted as described previously (22, 29). Serial transverse cryosections (16 μm) were stained with 0.1% thionin in acetate buffer (pH 3.9) to identify crural flexor motor neurons in the mouse lumbar spinal cord (L4-L5). Spinal cords were imaged using an Aperio ScanScope XT (Aperio) at ×20 magnification.

Skeletal muscle whole-mount immunofluorescence

Whole-mount immunofluorescence and analysis of NMJ innervation were conducted in the gastrocnemius of WT and hSOD1^{G93A} mice (22, 29). Alexa 555-α-bungarotoxin was used to localize AChRs (B35451; Invitrogen). A cocktail of antisynaptophysin (18-0130; Invitrogen) and antineurofilament (N4142; Sigma) was used to detect the presynaptic nerve terminal and axonal branches. Antisynaptophysin and antineurofilament were detected with an Alexa 488 goat antirabbit secondary antibody (A-11034; Invitrogen). Whole-mount muscles were imaged with a Zeiss LSM Meta 510 upright confocal microscope using a Plan-Apochromat ×40 oil objective (NA = 1.3; Carl Zeiss Inc).

Data and statistical analysis

The kinetics and secretory patterns of pulsatile GH secretion were determined by deconvolution analysis following parameters established previously (22, 32, 33). Approximate entropy of pulsatile GH secretion is considered to be regular when the P value is at .35 or below, and progressively less regular as the P value approaches 1. Correlation analyses were determined by linear regression and a Spearman correlation coefficient using GraphPad Prism 6.0c (GraphPad Inc). Differences between groups were limited to age-matched controls, and significant differences were identified by unpaired two-tailed Student's t test using GraphPad Prism 6.0c (GraphPad Inc). Data are presented as mean ± SEM. The threshold level for statistical significance was set at $P < .05$.

Results

Experiment 1: Disease progression specific changes in the GH/IGF-I axis in ALS in hSOD1^{G93A} mice

Motor neuron numbers and neuromuscular innervation are reduced in hSOD1^{G93A} mice at the onset stage of disease

ALS is characterized by the irreversible loss of upper (cortical) and lower motor neurons (2, 34, 35). The loss of motor neurons is reflected by a loss in motor unit number throughout the course of disease (29, 36, 37). This is accompanied by the progressive loss of innervation of NMJs in skeletal muscle (29), and compensatory axonal sprouting leading to reinnervation (27). We previously described a significant loss of crural flexor motor neurons and NMJ innervation in hSOD1^{G93A} mice at the latter stages of disease (22). To confirm histopathological changes in hSOD1^{G93A} mice, we quantified crural flexor motor neurons and NMJ innervation in presymptomatic hSOD1^{G93A} mice that had no signs of disease, and in hSOD1^{G93A} mice that had just developed hind limb weakness (Onset). These distinct disease stages have been characterized previously (29) and provide histolog-

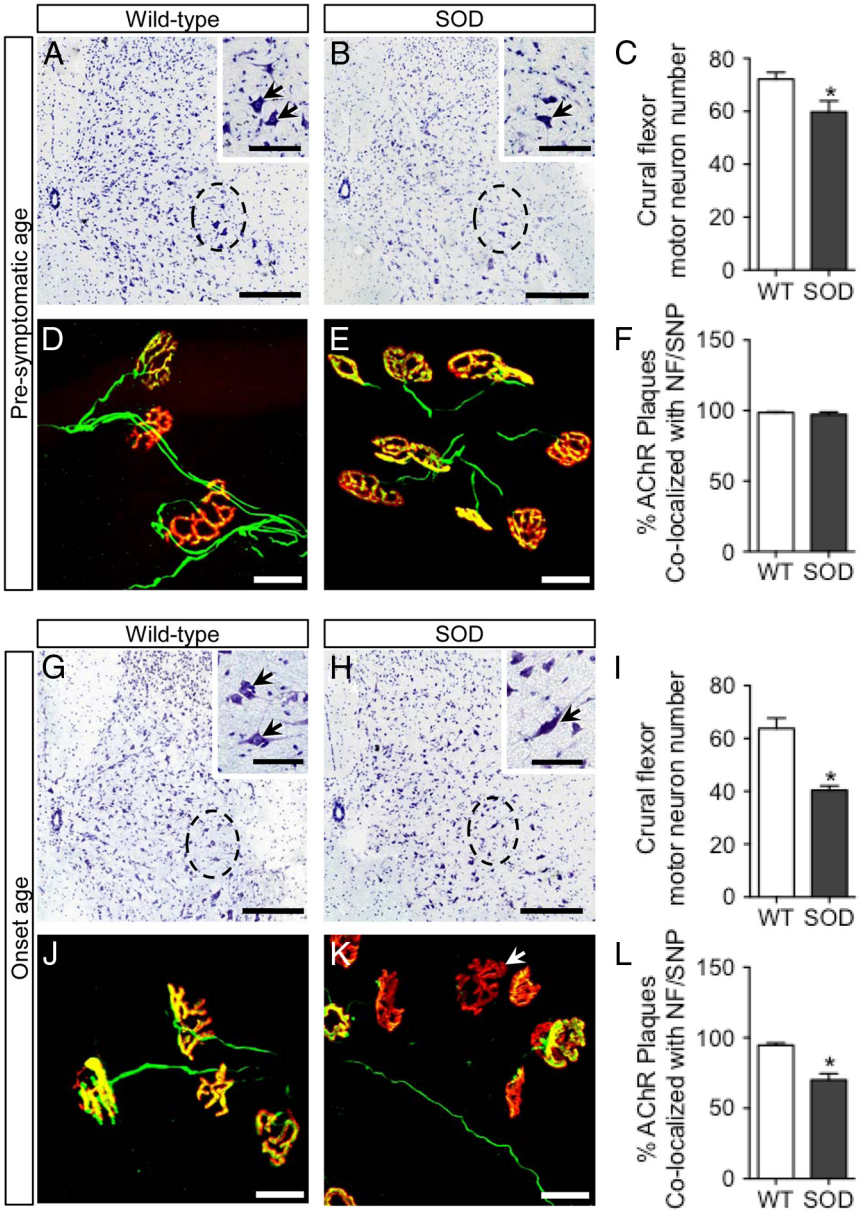

Figure 1. Histopathological assessment of disease progression in hSOD1^{G93A} mice by quantification of crural flexor motor neuron number (A–C and G–I) and NMJ innervation of the gastrocnemii (D–F and J–L) of hSOD1^{G93A} mice at an age prior to the development of overt symptoms (Presymptomatic age, 30–36 d old; A–F), and at an age associated with the onset of hind limb weakness (Onset age, 63 to 75 d old; G–L). Compared with age-matched WT controls, presymptomatic hSOD1^{G93A} mice had a modest yet significant reduction in the number of crural flexor motor neurons (A–C, black arrows), whereas NMJ innervation remained unchanged (D–F). At the onset stage of disease, hSOD1^{G93A} mice displayed a significant decrease in crural flexor motor neuron number (G–I, black arrows) and NMJ innervation (J–L, white arrows). NMJ innervation was assessed by the proportion of coexpression of AChR plaques (red signal) with neurofilament (NF) and synaptophysin (SNP) -positive nerve axons and terminals (green signal). *Insets of* A, B, G, and H illustrate a magnified view of the spinal cord region of interest (area containing the crural flexor motor neuron pool). *Scale bar* (A, B, G, and H), 250 μm and 100 μm for insets. *Scale bar* (D, E, J, and K), 100 μm. Values are expressed as mean ± SEM. $P < .05$ was accepted as significant; n = 5–6/group.

ical criteria for accurate assessment of disease progression. When compared with age-matched WT controls, presymptomatic hSOD1^{G93A} mice had a modest yet significant reduction in the number of crural flexor motor neurons (Figure 1, A–C), whereas neuromuscular innervation was unchanged (Figure 1, D–F), indicative of compensatory reinnervation. At the onset stage of disease, hSOD1^{G93A} mice displayed a significant decrease in crural flexor motor neuron number (Figure 1, G–I) and NMJ innervation of the muscle (Figure 1, J–L). Our data are congruent with previous observations of the progressive loss of motor neurons and loss of NMJ innervation in hSOD1^{G93A} mice (28, 29) and in ALS patients (38–40).

Pulsatile GH secretion is altered throughout disease progression in hSOD1^{G93A} mice

Having established that GH deficiency in human ALS (19, 20) is similar to that in end-stage hSOD1^{G93A} mice (22), we aimed to investigate the possible role of altered GH secretion in disease pathogenesis. We assessed pulsatile GH secretion in hSOD1^{G93A} mice at ages that reflect the presymptomatic, onset, and end stage of disease. Measures of pulsatile GH secretion in hSOD1^{G93A} mice were compared with that of age-matched WT controls. At all ages, pulsatile GH secretion was characterized by peak periods of GH secretion, flanked by periods of low basal secretion (Figure 2). Deconvolution analysis of GH secretion profiles between presymptomatic hSOD1^{G93A} animals and WT age-matched controls confirmed no differences in any parameters of pulsatile GH secretion (Table 1, Presymptomatic age). We observed significantly elevated total, pulsatile, and the mass per pulse (MPP) of GH secretion in hSOD1^{G93A} mice at disease onset when compared with WT age-matched controls (Table 1, Onset age). As demonstrated previously (22), we observed a significant reduction in total and pulsatile GH secretion, and the MPP of GH secretion in end-stage hSOD1^{G93A} mice when compared with WT age-matched controls (Table 1, End-stage

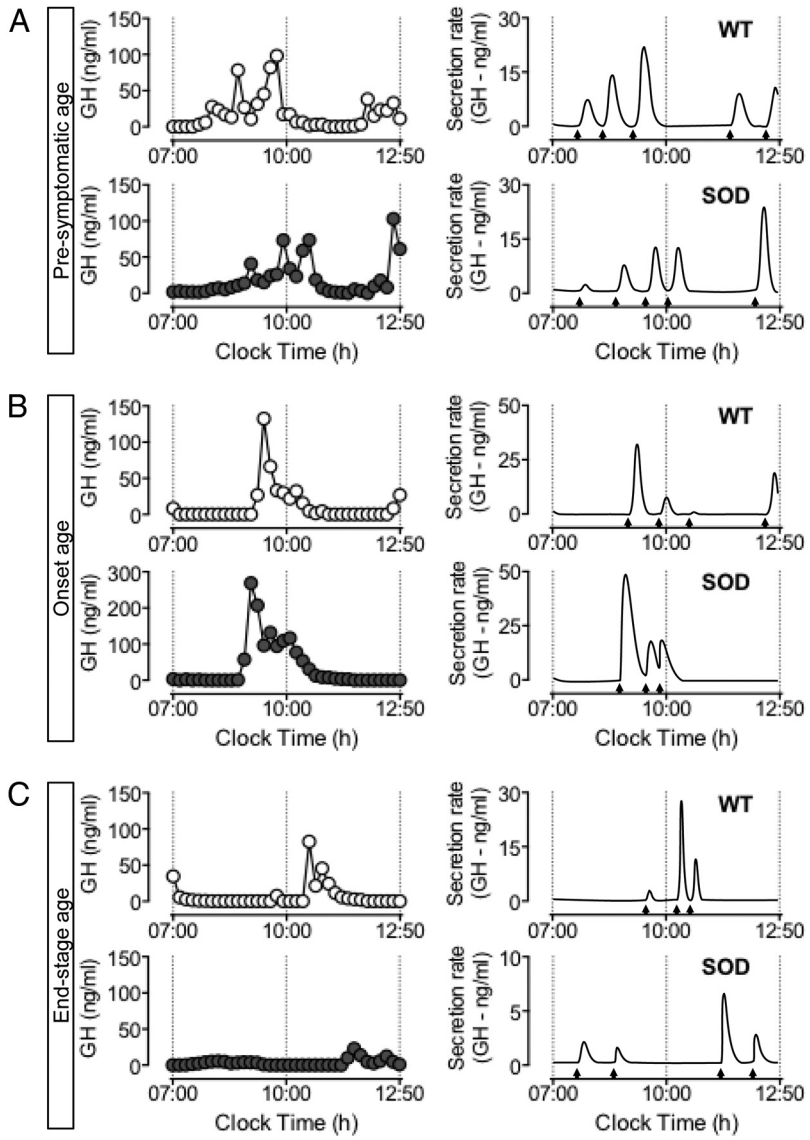

Figure 2. Pulsatile GH secretion in age-matched WT (open circles) mice, and in hSOD1^{G93A} mice (SOD, shaded circles) at ages corresponding to the presymptomatic (A; Presymptomatic age, 30–36 d old), onset (B; Onset age, 63 to 75 d old), and end stage (C; End-stage age; 150–175 d) of disease progression. Graphs illustrate representative examples from a single animal (left column) and resulting output figures demonstrating GH secretion rate (right column). Samples were collected for 6 hours at 10-minute intervals starting at 0700 hours. A regular periodicity of pulsatile GH secretion was characterized by peak secretion periods dispersed between stable low baseline secretion periods. Pulsatile GH secretion in SOD mice remained unchanged prior to disease onset (A), was elevated at disease onset (B), and was reduced at disease end stage (C) (data summarized in Table 1). The onset of pulses, as identified by deconvolution analysis, is illustrated along the x-axis of the output figures (black arrows).

age). Our observations thus reveal normal endogenous release of GH in presymptomatic hSOD1^{G93A} mice (regardless of the initial loss of motor neurons, Figure 1), elevated endogenous pulsatile GH secretion at the time of disease symptom onset when there is a significant loss of NMJ innervation of skeletal muscle (Figure 1), and the reduction in endogenous pulsatile GH secretion at the latter stage of disease progression.

Altered pulsatile GH secretion at disease onset in hSOD1^{G93A} mice coincides with altered Ghrh mRNA expression

In response to GH feedback, SRIF and GHRH inhibit and stimulate GH release, respectively (41). Assessment of Srif and Ghrh mRNA expression within the hypothalamus of hSOD1^{G93A} and WT animals at an age reflecting the onset of disease demonstrates no significant alterations in hypothalamic feedback that may account for increased GH release at this time. Rather, we observed a significant decline in Ghrh mRNA expression, whereas Srif mRNA expression remained unchanged (Figure 3, A and B). The decline in Ghrh mRNA, and presumably the eventual reduction in GHRH-induced GH production, may contribute to the observed reduction in pituitary GH content at the latter stage of disease progression (Figure 3C). Although speculative, data suggest that the factors accounting for enhanced GH release at disease onset do not act at the level of the hypothalamus.

Altered pulsatile GH secretion is not associated with changes in expression of skeletal muscle GH-R

GH exerts its anabolic effects directly at the level of skeletal muscle by signaling through the GH-R (42, 43). The irreversible loss of motor neurons in hSOD1^{G93A} mice throughout disease (28) occurs in parallel with pathological changes in skeletal muscle, including muscle atrophy (44, 45) and loss of NMJ innervation (29, 45). Thus, we asked whether altered GH secretion at the time of skeletal muscle denervation might result in altered GH-R expression in skeletal muscle as a means to compensate for muscle pathology. We determined the expression of Gh-r mRNA and GH-R protein in skeletal muscle of WT and hSOD1^{G93A} mice at ages that corresponded to presymptomatic, onset, and end stage of disease. Compared with age-matched WT con-

Table 1. Deconvolution Analysis Parameters of Pulsatile GH Secretion From Age-Matched Wild Type Controls and hSOD1^{G93A} Mice at an Age Prior to the Development of Disease Symptoms (Presymptomatic), at an Age Corresponding to the Appearance of Disease Symptoms (Onset), and at an Age Corresponding to Severe Disease Symptoms (End Stage)

	WT (n = 8)	SOD (n = 6)	*P* Value
Presymptomatic (30–36 d old)			
Total GH secretion, ng/mL/6 h	895 ± 116	1192 ± 324	.35
Pulsatile GH secretion rate, ng/mL/6 h	802 ± 92.0	1091 ± 292	.31
Mass of GH secreted/pulse (MPP), ng/mL	184 ± 42.8	231 ± 84.2	.60
Basal GH secretion rate, ng/mL/6 h	93.0 ± 32.8	99.4 ± 48.0	.91
Number of pulses/6 h	5.13 ± 0.58	5.88 ± 0.60	.42
Onset (63–75 d old)			
Total GH secretion, ng/mL/6 h	494 ± 52.0	1308 ± 301	.01[a]
Pulsatile GH secretion rate, ng/mL/6 h	451 ± 50.6	1214 ± 300	.01[a]
Mass of GH secreted/pulse (MPP), ng/mL	121 ± 18.1	424 ± 146	.04[a]
Basal GH secretion rate, ng/mL/6 h	43.1 ± 10.7	94.3 ± 41.3	.20
Number of pulses/6 h	3.88 ± 0.30	3.50 ± 0.56	.54
End stage (150–175 d old)			
Total GH secretion, ng/mL/6 h	583 ± 78.5	313 ± 32.8	.02[a]
Pulsatile GH secretion rate, ng/mL/6 h	526 ± 62.4	248 ± 44.6	<.01[a]
Mass of GH secreted/pulse (MPP), ng/mL	189 ± 32.1	70.4 ± 16.0	<.01[a]
Basal GH secretion rate, ng/mL/6 h	56.3 ± 19.5	65.4 ± 22.6	.77
Number of pulses/6 h	3.38 ± 0.38	3.83 ± 0.54	.49

Samples were collected at 10-minute intervals between 0700 h and 1300 h. Data are presented as mean ± SEM.
[a] $P < .05$ was considered significant.

trols, we observed no significant changes in protein (Figure 4, A and B) or gene (Figure 4C) expression of GH-R in hSOD1^{G93A} mice throughout disease. Observations suggest that, despite altered pulsatile GH secretion profiles, the capacity for GH to act on skeletal muscle in hSOD1^{G93A} mice is not altered.

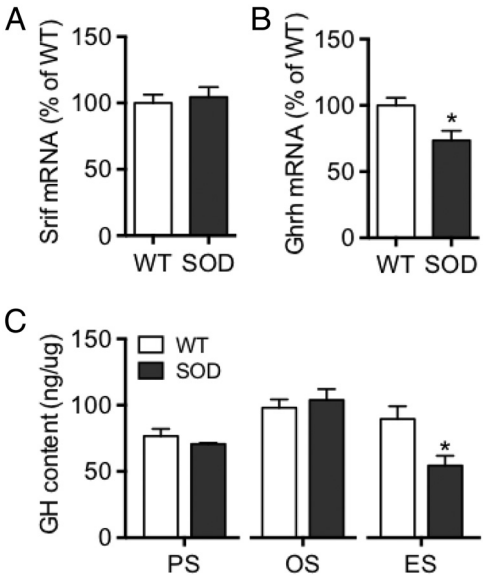

Figure 3. Hypothalamic Srif (A) and Ghrh (B) mRNA expression in age-matched WT and hSOD1^{G93A} (SOD) mice at disease onset (63 to 75 d old), and pituitary GH content (C) in WT and SOD mice at ages corresponding to the presymptomatic (PS, 30–36 d old), onset (OS, 63 to 75 d old), and end stage (ES; 150–175 d) ages of disease progression. No change in the expression of hypothalamic Srif mRNA was observed, whereas Ghrh mRNA expression declined significantly relative to age-matched WT controls. Pituitary GH content remained unchanged at disease onset; however, it declined significantly toward the latter stage of disease progression. Values are expressed as mean ± SEM. A value of $P < .05$ was accepted as significant; n = 6/group.

Disease progression–specific changes in GH secretion in hSOD1^{G93A} mice occur alongside an alteration in muscle specific but not circulating levels of IGF-I

The consequences of altered GH secretion throughout disease may be reflected by changes in IGF-I or IGF-IR expression. Although the actions of IGF-I are widespread (46–50), circulating IGF-I may inhibit GH production by negative feedback to the hypothalamus and anterior pituitary gland (48). Moreover, peak levels of GH are positively correlated to the production and release of IGF-I (51, 52). We have previously shown that diminished pulsatile GH secretion in hSOD1^{G93A} mice at the latter stages of disease occurs alongside a reduction in circulating levels of IGF-I, normal skeletal muscle IGF-I, and a decrease in the expression of muscle-specific IGF-IRα (22). Thus, we sought to determine circulating levels of IGF-I, and skeletal muscle expression of IGF-I, IGF-IRα, and IGF-IRβ protein in hSOD1^{G93A} mice at the presymptomatic and onset stages of disease. We found no difference in the expression of circulating IGF-I (Figure 5A), and skeletal muscle IGF-I (Figure 5B), IGF-IRα (Figure 5, C and D), and IGF-IRβ (Figure 5, E and F) protein in presymptomatic hSOD1^{G93A} mice when compared with WT age-matched controls. Similarly, we observed no significant change in the expression of circulating levels of IGF-I (Figure 5A), IGF-IRα (Figure 5, C and D), or IGF-IRβ (Figure 5, E and F) protein in skeletal muscle of hSOD1^{G93A} mice

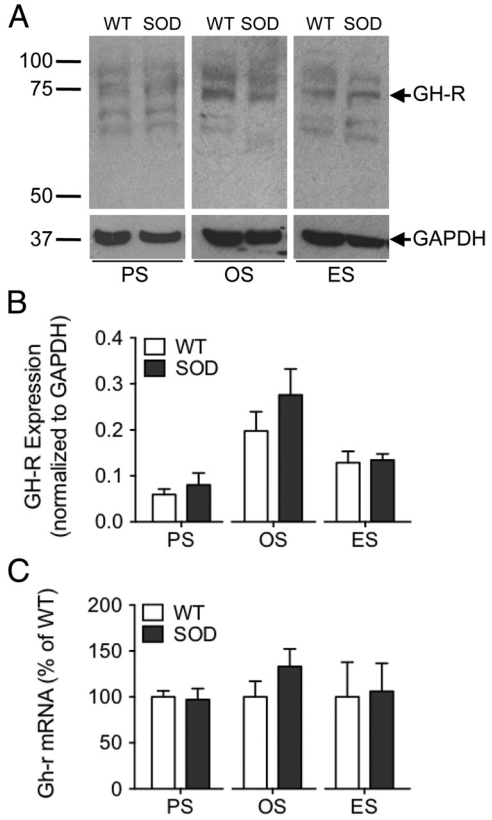

Figure 4. GH-R protein (A and B) and gene (C) expression in age-matched WT and hSOD1^{G93A} (SOD) mice at ages corresponding to the presymptomatic (PS, 30–36 d old), onset (OS, 63 to 75 d old), and end stage (ES; 150–175 d) ages of disease progression. No change in the expression of muscle GH-R was observed in SOD mice throughout disease. For protein expression, assessment was limited to the band corresponding to 71 kDa (A). The GH-R band was normalized to the GAPDH band. Given appearance of multiple protein bands, the lack of change in GH-R expression was confirmed by quantitative PCR for Gh-r mRNA (C). Values are expressed as mean ± SEM. A value of $P < .05$ was accepted as significant; n = 6/group.

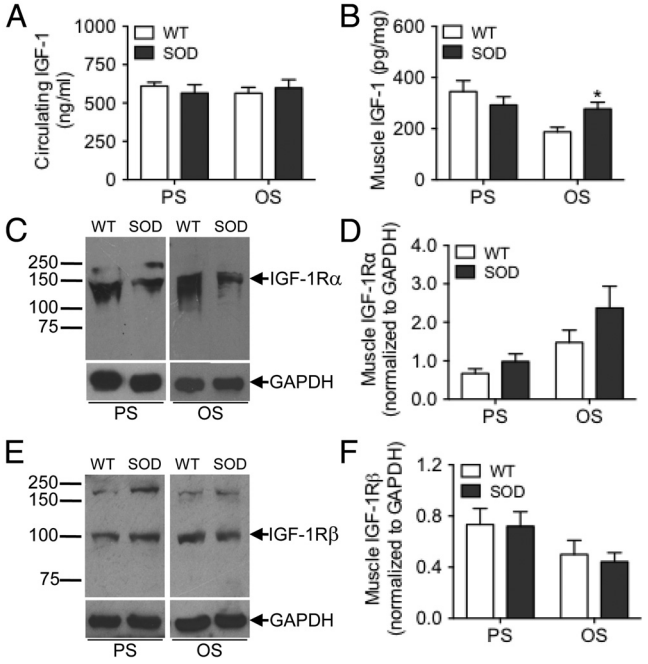

Figure 5. Circulating IGF-I (A), muscle-specific IGF-I (B), and muscle-specific IGF-IRα (C and D) and IGF-IRβ (E and F) expression in age-matched WT and hSOD1^{G93A} (SOD) mice at ages corresponding to the presymptomatic (PS, 30–36 d old) and onset (OS, 63 to 75 d old) stage of disease progression. No change in circulating IGF-I (A) or muscle-specific IGF-IRα and IGF-IRβ (C to F) expression was observed in PS or OS SOD mice. We observed a significant increase in muscle-specific IGF-I in SOD mice at an age corresponding to the OS of disease (B). For IGF-IRα (C) and IGF-IRβ (E), the IGF-IR band was normalized to the GAPDH band. Values are expressed as mean ± SEM. A value of $P < .05$ was accepted as significant; n = 6/group.

at the onset of disease. By contrast, the expression of muscle IGF-I protein in hSOD1^{G93A} mice was significantly higher at the onset stage of disease when compared with WT age-matched controls (Figure 5B).

Experiment 2: GH secretion in hSOD1^{G93A} mice at the onset of disease correlates with reduced NMJ denervation but not motor neuron survival

When compared with age-matched controls, an elevation in GH secretion was observed in hSOD1^{G93A} mice at the disease stage corresponding to the loss of motor neurons and reduced NMJ innervation (Onset; experiment 1). Thus, using a second cohort of hSOD1^{G93A} mice at the onset of disease symptoms, we next assessed the relationship between GH secretion and these histological hallmarks of disease. For each individual hSOD1^{G93A} animal, GH secretion profiles were correlated with the percentage of NMJ innervation and crural flexor motor neuron number from their gastrocnemius muscle and spinal cord.

In accordance with experiment 1, total, pulsatile, and MPP of GH secretion in hSOD1^{G93A} mice were elevated at the onset stage of disease when compared with age-matched WT mice (Table 2). Similarly, when compared with age-matched WT controls, we observed a decrease in the percentage of neuromuscular innervation and crural flexor motor neuron number. In hSOD1^{G93A} mice, Spearman correlation coefficient revealed that total and pulsatile GH secretion, and the MPP of GH secretion were positively correlated with the percentage of innervated NMJs; animals with higher levels of GH had less denervation. Crural flexor motor neuron number did not correlate with any of the parameters of pulsatile GH secretion. Representative examples of comparisons between total and pulsatile GH secretion, and the MPP of GH secretion relative to percentage NMJ innervation (Figure 6, A–C) and motor neuron count (Figure 6, D–F) are illustrated in Figure 6. All correlations are presented in Table 3.

Table 2. Histopathological Data (Crural Flexor Motor Neuron Number and Percentage NMJ Innervation), Deconvolution Analysis Parameters and Approximate Entropy Analysis Parameters of Pulsatile GH Secretion From C57Bl/6J and/or hSOD1^{G93A} Mice at an Age Corresponding to the Appearance of Disease Symptoms (Onset, 63 to 75 days of age)

	WT	SOD	*P* Value
Histopathological Data			
Motor neuron count	75.0 ± 5.18 (n = 6)	46.4 ± 5.19 (n = 12–16)	<.01[a]
% NMJ innervation	96.9 ± 1.14 (n = 6)	88.5 ± 3.21 (n = 12–16)	.03[a]
Measures of pulsatile GH release			
Total GH secretion, ng/mL/6 h	514 ± 73.8 (n = 6)	925 ± 146 (n = 16)	.01[a]
Pulsatile GH secretion rate, ng/mL/6 h	461 ± 64.7 (n = 6)	803 ± 144 (n = 16)	.04[a]
Mass of GH secreted/pulse (MPP), ng/mL	107 ± 12.2 (n = 6)	184 ± 29.2 (n = 16)	.04[a]
Basal GH secretion rate, ng/mL/6 h	52.6 ± 14.0 (n = 6)	105 ± 19.4 (n = 16)	.03[a]
Number of pulses/6 h	4.38 ± 0.32 (n = 6)	4.67 ± 0.38 (n = 16)	.57
Approximate entropy (1,0.35)	0.51 ± 0.05 (n = 6)	0.45 ± 0.04 (n = 16)	.34

For GH, samples were collected at 10-minute intervals between 0700 h and 1300 h. Data are presented as mean ± SEM.
[a] $P < .05$ was considered significant.

Discussion

ALS is a neurodegenerative disease, characterized by the irreversible death of upper (cortical) and lower motor neurons (1, 2). Although predominantly considered a neurological disorder, the dysregulation of multiple metabolic processes is thought to contribute to the rate of disease progression (14, 53). GH deficiency is observed in human ALS patients and mouse models of ALS (19, 22). However, the contribution of altered GH secretion to disease pathogenesis remains unknown. This is of particular interest, given that IGF-I-directed interventions prolong survival in a mouse model of ALS (54–56), whereas GH/IGF-I therapies were of no benefit in slowing disease progression in human ALS (21, 23–26). The discrepancy between these studies may occur as a consequence of species-specific differences in disease progression. Alternatively, disease stage-specific or tissue-specific interventions may have accounted for improved outcome in ALS mice. For example, effective IGF-I intervention in hSOD1^{G93A} mice occurred prior to the onset of disease pathology (55), or via administration of IGF-I to the central nervous system (57). To explain the striking differences in treatment outcomes between human trials and animal studies, it is essential that we understand the physiological changes in the GH/IGF-I axis throughout disease progression. Moreover, given that the existing treatment for ALS is largely ineffective, and that no cure currently exists for ALS, identification of key factors that modify the course of disease is of critical importance.

In this study, we first investigated the GH/IGF-I system in the hSOD1^{G93A} mouse at various stages of ALS disease progression. hSOD1^{G93A} mice showed alterations in GH secretion as disease symptoms and severity progressed. Relative to age-matched WT controls, we observed equivalent levels of GH secretion at an age reflecting the presymptomatic stage of disease, elevated GH secretion at the onset of disease symptoms, and GH deficiency at the latter stage of disease. When compared with age-matched con-

Table 3. Spearman Correlation Analysis of Deconvolution Parameters of Pulsatile GH Secretion With Percentage NMJ Innervation of the Gastrocnemius, and Crural Flexor Motor Neuron Number From C57Bl/6J and/or hSOD1^{G93A} Mice at an Age Corresponding to the Appearance of Disease Symptoms (Onset, 63 to 75 days of age).

	% NMJ Innervation (n = 16)		Motor Neuron Number (n = 12)	
	r	*P* Value	*r*	*P* Value
Spearman Correlation Analysis				
Total GH secretion, ng/mL/6 h	0.64	<.01[a]	−0.05	.44
Pulsatile GH secretion rate, ng/mL/6 h	0.69	<.01[a]	−0.06	.42
Mass of GH secreted/burst (MPP), ng/mL	0.82	<.01[a]	−0.23	.23
Basal GH secretion rate, ng/mL/6 h	0.09	.38	−0.20	.26
Number of pulses/6 h	−0.39	.06	−0.47	.06
Approximate entropy (1,0.35)	−0.31	.12	−0.25	.21

For GH, samples were collected at 10-minute intervals between 0700 h and 1300 h. Data are presented as mean ± SEM.
[a] $P < .05$ was considered significant.

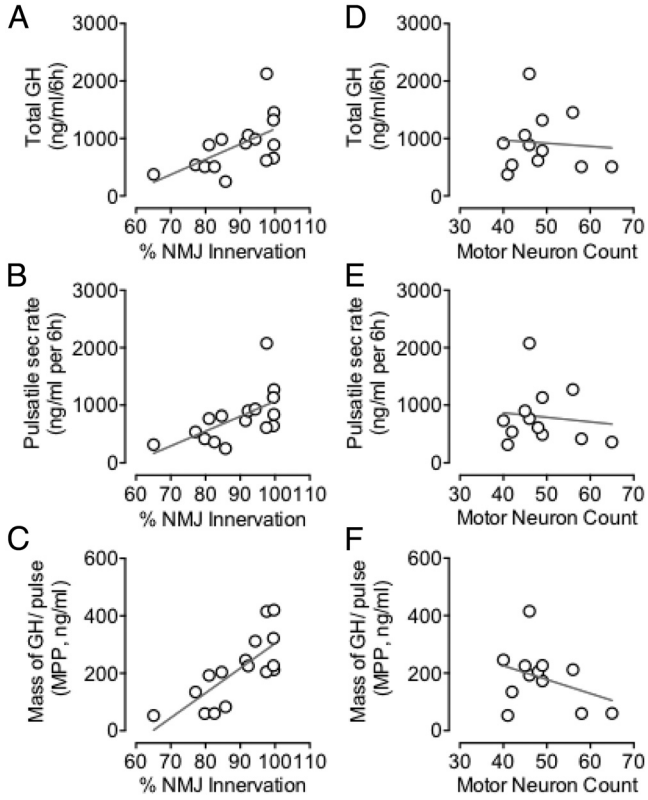

Figure 6. Representative examples of total (A and D), pulsatile (B and E), and mean mass per GH pulse (MPP; C and F) of GH secretion correlated to the percentage of innervated neuromuscular junctions (% NMJ Innervation) in gastrocnemii (A–C) and crural flexor motor neuron number (Motor Neuron Count) in L4–L5 of the lateral motor column (D–F) of respective hSOD1^{G93A} mice. Spearman correlation analysis was performed to assess the relationship between measures of pulsatile GH secretion following deconvolution analysis and percentage NMJ innervation and motor neuron count. Data for all parameters are summarized in Table 2 and 3. For %NMJ innervation, n = 16. For motor neuron count, n = 12.

trols, normal levels of circulating and muscle IGF-I, and muscle GH-R and IGF-IR (α and β subunit) protein, accompanied normal pulsatile GH secretion in hSOD1^{G93A} mice at the presymptomatic stage of disease. When compared with age-matched WT controls, hSOD1^{G93A} mice at disease onset had higher levels of pulsatile GH and muscle IGF-I protein expression, but normal circulating levels of IGF-I, and skeletal muscle GH-R and IGF-IR (α and β subtype) protein expression. By the end stage of disease in hSOD1^{G93A} mice, and despite GH deficiency, there was no change in skeletal muscle GH-R protein expression. We have previously shown that GH-deficient hSOD1^{G93A} mice at the end stage of disease have decreased circulating IGF-I, normal muscle IGF-I, and decreased skeletal muscle IGF-IRα (22). After characterizing GH secretion relative to disease progression, we assessed the relationship between GH secretion and histological hallmarks of disease in individual hSOD1^{G93A} mice at the onset of symptoms. Parameters of pulsatile GH secretion were positively correlated with the percentage of NMJ innervation (suggesting reinnervation has occurred to compensate for denervation) in skeletal muscle, but not with crural flexor motor neuron number. Taken together, our observations suggest that altered GH secretion and muscle IGF-I expression may reflect an endogenous endocrine response that serves to counteract the denervation that occurs in ALS, as it is known that IGF-I promotes axonal sprouting (58).

Although GH modulates the size and density of cortical neurons during development (59), it does not regulate the survival of motor neurons that innervate the hind limb (60). Thus, it is unlikely that GH alone would attenuate neuronal death in ALS. In line with this, GH therapy in ALS patients does not slow disease progression (21, 25), nor did we observe alterations in GH release relative to motor neuron death. When compared with age-matched WT controls, presymptomatic hSOD1^{G93A} mice had reduced crural flexor motor neuron numbers, whereas the secretion of GH did not change. Moreover, given that parameters of pulsatile GH secretion did not correlate with crural flexor motor neuron number in hSOD1^{G93A} mice at the onset of disease, we conclude that altered GH release does not specifically occur as a consequence of motor neuron loss. If not neuronal death, does muscle pathology in ALS contribute to altered GH release?

If changes in GH/IGF-I were a consequence of muscle pathology, it may be expected that the first observable differences in GH/IGF-I would occur when the loss of NMJs first manifest. In this instance, we demonstrate altered GH release alongside NMJ denervation. As documented (29, 61), NMJ denervation in hSOD1^{G93A} mice occurs at symptom onset, or at a slightly earlier age (29, 61). The delay between motor neuron loss and the loss of NMJ innervation is thought to occur in response to early compensatory adaptive collateral sprouting of motor axons, which promotes the reinnervation of denervated muscle (27). Once adaptive sprouting reaches a critical threshold, maladaptive sprouting results in an inability to compensate for further neuromuscular denervation (27), resulting in the loss of innervation. Not surprisingly, muscle weakness and atrophy in ALS are attributed to this significant loss of neuromuscular innervation (39). Thus, it is plausible that on the loss of a critical number of NMJs (29), the GH/IGF-I axis may compensate by promoting muscle mass and hypertrophy (17, 62), and by attempting to drive axonal sprouting further to preserve remaining muscle function (46, 47). Alternatively, activation of the GH/IGF-I axis may occur much earlier and may precede sprouting. Of interest, GH secretion in WT animals declined between 5 to 10 weeks of age, whereas this age-associated decline in GH secretion was not observed in hSOD1^{G93A} mice between the presymptomatic and onset

stages of disease. This observation is reflected by the maintenance of muscle IGF-I expression in hSOD1^{G93A} mice at the onset stage of disease. Thus, whether the altered GH/IGF-I profile in hSOD1^{G93A} mice observed at the onset of disease results from GH hypersecretion or is a reflection of the prevention of the age-associated decline GH secretion remains to be determined. Future studies that define the parameters of GH secretion in hSOD1^{G93A} mice between the presymptomatic and onset stages of disease will provide insight into the mechanisms that underlie this unique GH/IGF-I profile. More importantly, these observations may provide key insights to couple GH release and compensatory adaptive collateral sprouting of motor axons in ALS.

We observe no difference in the expression of circulating IGF-I between hSOD1^{G93A} mice and age-matched WT controls at ages that corresponded to the presymptomatic and onset stage of disease. This is consistent with reports in human ALS, which describe equivalent levels of IGF-I between ALS patients and controls in the absence of confirmed GH deficiency (21). These observations, taken with our previous reports of reduced circulating IGF-I in GH-deficient hSOD1^{G93A} mice at the end stage of disease (22), and a trend toward lower IGF-I in GH-deficient ALS patients (19), suggest that circulating IGF-I may not act as a neuroprotective factor in ALS. Conversely, GH drives tissue-specific production of IGF-I (48), whereas muscle IGF-I promotes axonal sprouting (46, 47). Thus, although GH itself appears to have no neuroprotective role, the protective capacity of the GH/IGF-I axis may lie in the early overexpression of tissue-specific IGF-I. Indeed, delivery of IGF-I into the spinal cord of animal models of ALS prolongs survival (57), improves motor function, and attenuates motor neuron loss (63, 64). Similarly, early retrograde delivery of IGF-I via im injection prolongs survival (56), and embryonic overexpression of IGF-I in skeletal muscle prevents motor neuron loss in ALS mice (55). In line with the argument that beneficial effects from IGF-I specifically require early and tissue-specific treatment, subcutaneous administration of IGF-I in ALS patients well after the onset of disease symptoms has resulted in minimal benefit (23, 26).

The mechanisms underlying altered GH release in symptomatic hSOD1^{G93A} mice remain unknown. In this regard, a feedback mechanism may exist in ALS, wherein a muscle-derived factor (produced in response to early denervation and/or maladaptive sprouting) may modulate hypothalamic and/or pituitary-mediated GH release. We observed a reduction in hypothalamic Ghrh mRNA expression in hSOD1^{G93A} mice at an age reflecting disease onset. Given established feedback mechanisms whereby GH suppresses central GHRH-induced GH release (41), the observed reduction in Ghrh mRNA expression is likely a consequence of high levels of endogenous GH secretion. Thus, one may speculate that the GH secretion profile, specific to disease onset, occurs in response to circulating factors acting specifically at the level of the anterior pituitary gland. Moreover, prolonged suppression of GHRH activity may eventuate in an overall reduction in GHRH-induced GH production and may account for the eventual depletion of pituitary GH content in hSOD1^{G93A} mice at the end stage of disease (22). This requires further investigation. Moreover, the secretion of a muscle-derived factor that influences the amplitude of GH release in ALS, through central or peripheral mechanisms, presents an interesting avenue for further assessment.

This study is the first to investigate the GH/IGF-I axis throughout disease progression in ALS mice. Alterations in circulating and muscle IGF-I in hSOD1^{G93A} mice are reflective of the endogenous GH profile. The positive correlation between circulating levels of GH and neuromuscular innervation (ie, reduced denervation) in hSOD1^{G93A} mice at the onset of disease imply that primary changes to the GH/IGF-I axis are a physiological response to compensate for, and potentially to minimize the morbidity of, disease at the earlier stages of the disease process (when muscle pathology is less severe). Subsequent GH deficiency and decreased circulating IGF-I (22) may result from the ongoing disease process, when severe histological pathology inherent to ALS (inexorable motor neuron loss and coincident muscle weakness and atrophy due to an inability to maintain collateral sprouting of axons) are prominent. Current measures provide insight into the role of the endogenous GH/IGF-I response in disease progression in ALS. Despite the benefits of IGF-I treatment in ALS mice (54–56), the inability for elevated and/or sustained levels of endogenous GH and muscle IGF-I to attenuate motor neuron loss and neuromuscular denervation in hSOD1^{G93A} mice throughout disease is not supportive of a neuroprotective role of endogenous GH/IGF-I in ALS.

Acknowledgments

The authors dedicate this manuscript to Mr Scott Sullivan and Dr Ian Davis and their efforts in raising awareness and research funding for ALS. We thank Dr Lili Huang, Ms Hwee Tan, Ms Teresa Xie, and Ms Ying Wan for their technical assistance. This research was supported by the Australian National Health and Medical Research Council, The University of Queensland, and the Motor Neurone Disease Research Institute of Australia. S.T.N. is supported by a Bill Gole Fellowship from the Motor Neurone Disease Research Institute of Australia. K.L. is the recipient of an Australian Post-graduate Award Postgraduate

Scholarship from the Australian Government Department of Industry, Innovation Science, Research, and Tertiary Education.

Address all correspondence and requests for reprints to: Dr Shyuan Ngo, School of Biomedical Sciences, University of Queensland, St Lucia 4072, Australia. E-mail: s.ngo@uq.edu.au; or Prof Chen Chen, School of Biomedical Sciences, University of Queensland, St Lucia 4072, Australia. E-mail: chen.chen@uq.edu.au.

Disclosure Summary: The authors have nothing to disclose.

References

1. **Cleveland DW, Rothstein JD.** From Charcot to Lou Gehrig: deciphering selective motor neuron death in ALS. *Nat Rev Neurosci*. 2001;2:806–819.
2. **Mitchell JD, Borasio GD.** Amyotrophic lateral sclerosis. *Lancet*. 2007;369:2031–2041.
3. **Blair IP, Williams KL, Warraich ST, et al.** FUS mutations in amyotrophic lateral sclerosis: clinical, pathological, neurophysiological and genetic analysis. *J Neurol Neurosurg Psychiatry*. 2010;81:639–645.
4. **DeJesus-Hernandez M, Mackenzie IR, Boeve BF, et al.** Expanded GGGGCC hexanucleotide repeat in noncoding region of C9ORF72 causes chromosome 9p-linked FTD and ALS. *Neuron*. 2011;72:245–256.
5. **Kabashi E, Valdmanis PN, Dion P, et al.** TARDBP mutations in individuals with sporadic and familial amyotrophic lateral sclerosis. *Nat Genet*. 2008;40:572–574.
6. **Maruyama H, Morino H, Ito H, et al.** Mutations of optineurin in amyotrophic lateral sclerosis. *Nature*. 2010;465:223–226.
7. **Orrell RW.** Motor neuron disease: systematic reviews of treatment for ALS and SMA. *Br Med Bull*. 2010;93:145–159.
8. **Renton AE, Majounie E, Waite A, et al.** A hexanucleotide repeat expansion in C9ORF72 is the cause of chromosome 9p21-linked ALS-FTD. *Neuron*. 2011;72:257–268.
9. **Rothstein JD.** Current hypotheses for the underlying biology of amyotrophic lateral sclerosis. *Ann Neurol 65 Suppl*. 2009;1:S3–S9.
10. **Bendotti C, Calvaresi N, Chiveri L, et al.** Early vacuolization and mitochondrial damage in motor neurons of FALS mice are not associated with apoptosis or with changes in cytochrome oxidase histochemical reactivity. *J Neurol Sci*. 2001;191:25–33.
11. **Crugnola V, Lamperti C, Lucchini V, et al.** Mitochondrial respiratory chain dysfunction in muscle from patients with amyotrophic lateral sclerosis. *Arch Neurol*. 2010;67:849–854.
12. **Zhou J, Yi J, Fu R, et al.** Hyperactive intracellular calcium signaling associated with localized mitochondrial defects in skeletal muscle of an animal model of amyotrophic lateral sclerosis. *J Biol Chem*. 2010;285:705–712.
13. **Dupuis L, Oudart H, René F, Gonzalez de Aguilar JL, Loeffler JP.** Evidence for defective energy homeostasis in amyotrophic lateral sclerosis: benefit of a high-energy diet in a transgenic mouse model. *Proc Natl Acad Sci U S A*. 2004;101:11159–11164.
14. **Dupuis L, Pradat PF, Ludolph AC, Loeffler JP.** Energy metabolism in amyotrophic lateral sclerosis. *Lancet Neurol*. 2011;10:75–82.
15. **Fergani A, Oudart H, Gonzalez De Aguilar JL, et al.** Increased peripheral lipid clearance in an animal model of amyotrophic lateral sclerosis. *J Lipid Res*. 2007;48:1571–1580.
16. **Phatnani HP, Guarnieri P, Friedman BA, et al.** Intricate interplay between astrocytes and motor neurons in ALS. *Proc Natl Acad Sci U S A*. 2013;110:E756–E765.
17. **Jørgensen JO, Rubeck KZ, Nielsen TS, et al.** Effects of GH in human muscle and fat. *Pediatr Nephrol*. 2010;25:705–709.
18. **Møller N, Jørgensen JO.** Effects of growth hormone on glucose, lipid, and protein metabolism in human subjects. *Endocr Rev*. 2009;30:152–177.
19. **Morselli LL, Bongioanni P, Genovesi M, et al.** Growth hormone secretion is impaired in amyotrophic lateral sclerosis. *Clin Endocrinol*. 2006;65:385–388.
20. **Pellecchia MT, Pivonello R, Monsurrò MR, et al.** The GH-IGF system in amyotrophic lateral sclerosis: correlations between pituitary GH secretion capacity, insulin-like growth factors and clinical features. *Eur J Neurol*. 2010;17:666–671.
21. **Saccà F, Quarantelli M, Rinaldi C, et al.** A randomized controlled clinical trial of growth hormone in amyotrophic lateral sclerosis: clinical, neuroimaging, and hormonal results. *J Neurol*. 2012;259:132–138.
22. **Steyn FJ, Ngo ST, Lee JD, et al.** Impairments to the GH-IGF-I axis in hSOD1G93A mice give insight into possible mechanisms of GH dysregulation in patients with amyotrophic lateral sclerosis. *Endocrinology*. 2012;153:3735–3746.
23. **Borasio GD, Robberecht W, Leigh PN, et al.** A placebo-controlled trial of insulin-like growth factor-I in amyotrophic lateral sclerosis. European ALS/IGF-I Study Group. *Neurology*. 1998;51:583–586.
24. **Lai EC, Felice KJ, Festoff BW, et al.** Effect of recombinant human insulin-like growth factor-I on progression of ALS. A placebo-controlled study. The North America ALS/IGF-I Study Group. *Neurology*. 1997;49:1621–1630.
25. **Smith RA, Melmed S, Sherman B, Frane J, Munsat TL, Festoff BW.** Recombinant growth hormone treatment of amyotrophic lateral sclerosis. *Muscle Nerve*. 1993;16:624–633.
26. **Sorenson EJ, Windbank AJ, Mandrekar JN, et al.** Subcutaneous IGF-1 is not beneficial in 2-year ALS trial. *Neurology*. 2008;71:1770–1775.
27. **Gordon T, Hegedus J, Tam SL.** Adaptive and maladaptive motor axonal sprouting in aging and motoneuron disease. *Neurol Res*. 2004;26:174–185.
28. **Gurney ME, Pu H, Chiu AY, et al.** Motor neuron degeneration in mice that express a human Cu,Zn superoxide dismutase mutation. *Science*. 1994;264:1772–1775.
29. **Ngo ST, Baumann F, Ridall PG, et al.** The relationship between Bayesian motor unit number estimation and histological measurements of motor neurons in wild-type and SOD1(G93A) mice. *Clin Neurophysiol*. 2012;123:2080–2091.
30. **Steyn FJ, Huang L, Ngo ST, et al.** Development of a method for the determination of pulsatile growth hormone secretion in mice. *Endocrinology*. 2011;152:3165–3171.
31. **Ngo ST, Cole RN, Sunn N, Phillips WD, Noakes PG.** Neuregulin-1 potentiates agrin-induced acetylcholine receptor clustering through muscle-specific kinase phosphorylation. *J Cell Sci*. 2012;125:1531–1543.
32. **Keenan DM, Chattopadhyay S, Veldhuis JD.** Composite model of time-varying appearance and disappearance of neurohormone pulse signals in blood. *J Theor Biol*. 2005;236:242–255.
33. **Keenan DM, Iranmanesh A, Veldhuis JD.** Analytical construct of reversible desensitization of pituitary-testicular signaling: illustrative application in aging. *Am J Physiol Regul Integr Comp Physiol*. 2011;300:R349–R360.
34. **Magnus T, Beck M, Giess R, Puls I, Naumann M, Toyka KV.** Disease progression in amyotrophic lateral sclerosis: predictors of survival. *Muscle Nerve*. 2002;25:709–714.
35. **Rowland LP, Shneider LA.** Amyotrophic lateral sclerosis. *N Engl J Med*. 2001;344:1688–1700.
36. **Baumann F, Henderson RD, Gareth Ridall P, Pettitt AN, McCombe PA.** Quantitative studies of lower motor neuron degeneration in amyotrophic lateral sclerosis: evidence for exponential decay of motor unit numbers and greatest rate of loss at the site of onset. *Clin Neurophysiol*. 2012;123:2092–2098.
37. **Baumann F, Henderson RD, Ridall PG, Pettitt AN, McCombe PA.** Use of Bayesian MUNE to show differing rate of loss of motor units in subgroups of ALS. *Clin Neurophysiol*. 2012;123:2446–2453.

38. **Ekegren T, Grundström E, Lindholm D, Aquilonius SM.** Upregulation of Bax protein and increased DNA degradation in ALS spinal cord motor neurons. *Acta Neurol Scand*. 1999;100:317–321.
39. **Maselli RA, Wollman RL, Leung C, et al.** Neuromuscular transmission in amyotrophic lateral sclerosis. *Muscle Nerve*. 1993;16: 1193–1203.
40. **Swash M, Leader M, Brown A, Swettenham KW.** Focal loss of anterior horn cells in the cervical cord in motor neuron disease. *Brain*. 1986;109 (Pt 5):939–952.
41. **Müller EE, Locatelli V, Cocchi D.** Neuroendocrine control of growth hormone secretion. *Physiol Rev*. 1999;79:511–607.
42. **Mavalli MD, DiGirolamo DJ, Fan Y, et al.** Distinct growth hormone receptor signaling modes regulate skeletal muscle development and insulin sensitivity in mice. *J Clin Invest*. 2010;120:4007–4020.
43. **Sotiropoulos A, Ohanna M, Kedzia C, et al.** Growth hormone promotes skeletal muscle cell fusion independent of insulin-like growth factor 1 up-regulation. *Proc Natl Acad Sci U S A*. 2006;103:7315–7320.
44. **Léger B, Vergani L, Sorarù G, et al.** Human skeletal muscle atrophy in amyotrophic lateral sclerosis reveals a reduction in Akt and an increase in atrogin-1. *FASEB J*. 2006;20:583–585.
45. **Muller FL, Song W, Jang YC, et al.** Denervation-induced skeletal muscle atrophy is associated with increased mitochondrial ROS production. *Am J Physiol Regul Integr Comp Physiol*. 2007;293: R1159–R1168.
46. **Fryburg DA.** Insulin-like growth factor I exerts growth hormone- and insulin-like actions on human muscle protein metabolism. *Am J Physiol*. 1994;267:E331–E336.
47. **Fryburg DA, Jahn LA, Hill SA, Oliveras DM, Barrett EJ.** Insulin and insulin-like growth factor-I enhance human skeletal muscle protein anabolism during hyperaminoacidemia by different mechanisms. *J Clin Invest*. 1995;96:1722–1729.
48. **Le Roith D, Bondy C, Yakar S, Liu JL, Butler A.** The somatomedin hypothesis: 2001. *Endocr Rev*. 2001;22:53–74.
49. **Musarò A, Dobrowolny G, Rosenthal N.** The neuroprotective effects of a locally acting IGF-1 isoform. *Exp Gerontol*. 2007; 42:76–80.
50. **Svrzic D, Schubert D.** Insulin-like growth factor 1 supports embryonic nerve cell survival. *Biochem Biophys Res Commun*. 1990;172: 54–60.
51. **Isgaard J, Nilsson A, Vikman K, Isaksson OG.** Growth hormone regulates the level of insulin-like growth factor-I mRNA in rat skeletal muscle. *J Endocrinol*. 1989;120:107–112.
52. **Maiter D, Underwood LE, Maes M, Davenport ML, Ketelslegers JM.** Different effects of intermittent and continuous growth hormone (GH) administration on serum somatomedin-C/insulin-like growth factor I and liver GH receptors in hypophysectomized rats. *Endocrinology*. 1988;123:1053–1059.
53. **Robberecht W, Philips T.** The changing scene of amyotrophic lateral sclerosis. *Nat Rev Neurosci*. 2013;14:248–264.
54. **Dobrowolny G, Aucello M, Molinaro M, Musarò A.** Local expression of mIgf-1 modulates ubiquitin, caspase and CDK5 expression in skeletal muscle of an ALS mouse model. *Neurol Res*. 2008;30: 131–136.
55. **Dobrowolny G, Giacinti C, Pelosi L, et al.** Muscle expression of a local Igf-1 isoform protects motor neurons in an ALS mouse model. *J Cell Biol*. 2005;168:193–199.
56. **Kaspar BK, Lladó J, Sherkat N, Rothstein JD, Gage FH.** Retrograde viral delivery of IGF-1 prolongs survival in a mouse ALS model. *Science*. 2003;301:839–842.
57. **Dodge JC, Haidet AM, Yang W, et al.** Delivery of AAV-IGF-1 to the CNS extends survival in ALS mice through modification of aberrant glial cell activity. *Mol Ther*. 2008;16:1056–1064.
58. **Salie R, Steeves JD.** IGF-1 and BDNF promote chick bulbospinal neurite outgrowth in vitro. *Int J Dev Neurosci*. 2005;23:587–598.
59. **Ransome MI, Goldshmit Y, Bartlett PF, Waters MJ, Turnley AM.** Comparative analysis of CNS populations in knockout mice with altered growth hormone responsiveness. *Eur J Neurosci*. 2004;19: 2069–2079.
60. **Parsons SA, Banks GB, Rowland JA, et al.** Genetic disruption of the growth hormone receptor does not influence motoneuron survival in the developing mouse. *Int J Dev Biol*. 2003;47:41–49.
61. **Frey D, Schneider C, Xu L, Borg J, Spooren W, Caroni P.** Early and selective loss of neuromuscular synapse subtypes with low sprouting competence in motoneuron diseases. *J Neurosci*. 2000;20:2534–2542.
62. **Grounds MD.** Reasons for the degeneration of ageing skeletal muscle: a central role for IGF-1 signalling. *Biogerontology*. 2002; 3:19–24.
63. **Lepore AC, Haenggeli C, Gasmi M, et al.** Intraparenchymal spinal cord delivery of adeno-associated virus IGF-1 is protective in the SOD1G93A model of ALS. *Brain Res*. 2007;1185:256–265.
64. **Franz CK, Federici T, Yang J, et al.** Intraspinal cord delivery of IGF-I mediated by adeno-associated virus 2 is neuroprotective in a rat model of familial ALS. *Neurobiol Dis*. 2009;33:473–481.